

# Journal of Biomedical Optics

BiomedicalOptics.SPIEDigitalLibrary.org

## **Miniature probe for the delivery and monitoring of a photopolymerizable material**

Andreas Schmocker  
Azadeh Khoushabi  
Constantin Schizas  
Pierre-Etienne Bourban  
Dominique P. Pioletti  
Christophe Moser

# Miniature probe for the delivery and monitoring of a photopolymerizable material

Andreas Schmocker,<sup>a,b,\*</sup> Azadeh Khoushabi,<sup>b,c</sup> Constantin Schizas,<sup>d</sup> Pierre-Etienne Bourban,<sup>c</sup> Dominique P. Pioletti,<sup>b</sup> and Christophe Moser<sup>a</sup>

<sup>a</sup>Swiss Federal Institute of Technology Lausanne, Microengineering Institute, Laboratory of Applied Photonics Devices, Station 17, Lausanne 1015, Switzerland

<sup>b</sup>Swiss Federal Institute of Technology Lausanne, Institute of Bioengineering, Laboratory of Biomechanical Orthopedics, Station 19, Lausanne 1015, Switzerland

<sup>c</sup>Swiss Federal Institute of Technology Lausanne, Institute of Materials, Laboratory of Polymer and Composite Technology, Station 12, Lausanne 1015, Switzerland

<sup>d</sup>Clinic Cecil, Neuro-orthopedic Spine Unit, Avenue Louis-Ruchonnet 53, Lausanne 1003, Switzerland

**Abstract.** Photopolymerization is a common method to cure materials initially in a liquid state, such as dental implants or bone or tissue fillers. Recent advances in the development of biocompatible gel- and cement-systems open up an avenue for *in situ* photopolymerization. For minimally invasive surgery, such procedures require miniaturized surgical endoscopic probes to activate and control photopolymerization *in situ*. We present a miniaturized light probe in which a photoactive material can be (1) mixed, pressurized, and injected, (2) photopolymerized/photoactivated, and (3) monitored during the chemical reaction. The device is used to implant and cure poly(ethylene glycol) dimethacrylate-hydrogel-precursor *in situ* with ultraviolet A (UVA) light (365 nm) while the polymerization reaction is monitored in real time by collecting the fluorescence and Raman signals generated by the 532-nm excitation light source. Hydrogels could be delivered, photopolymerized, and monitored by the probe up to a curing depth of 4 cm. The size of the photopolymerized samples could be correlated to the fluorescent signal collected by the probe, and the reproducibility of the procedure could be demonstrated. The position of the probe tip inside a bovine caudal intervertebral disc could be estimated *in vitro* based on the collected fluorescence and Raman signal. © The Authors. Published by SPIE under a Creative Commons Attribution 3.0 Unported License. Distribution or reproduction of this work in whole or in part requires full attribution of the original publication, including its DOI. [DOI: 10.1117/1.JBO.20.12.127001]

Keywords: probe; polymerized medical implant; light scattering; cross-linking; injectable hydrogel; *in situ* photopolymerization; fluorescence spectroscopy; Raman spectroscopy; real-time monitoring.

Paper 150392R received Jun. 10, 2015; accepted for publication Oct. 30, 2015; published online Dec. 10, 2015.

## 1 Introduction

Photopolymerization<sup>1,2</sup> is widely used to harden polymers in controllable manner by illuminating a liquid monomer or an uncured polymer precursor. Initially, photopolymerization was used for coatings, printing, paints, adhesives, optical fibers, etch resist, or printed circuits.<sup>3–6</sup> It has found its way into the biomedical sector, where photopolymerizable materials are used for dental implants,<sup>7</sup> cell encapsulation,<sup>8,9</sup> tissue-replacements,<sup>10,11</sup> drug delivery,<sup>12</sup> implant coatings, bio-glues,<sup>13</sup> and microfluidics.<sup>14</sup> One of the advantages of photopolymerization is that by using light illumination, the initiation and speed of the polymerization reaction can be controlled actively.<sup>15</sup> To monitor photopolymerization reactions, methods such as speckle interferometry,<sup>16</sup> Raman spectroscopy,<sup>17</sup> transmittance measurements,<sup>18</sup> fluorescence spectroscopy,<sup>19–21</sup> UV-, Vis-, near-infrared (NIR)-, and mid-infrared (MIR)-spectroscopy, nuclear magnetic resonance spectroscopy, and acoustic monitoring<sup>22</sup> have been proposed.

However, during minimally invasive surgical implantation of a photopolymerizable material, the implant is hardly accessible, which makes the methods above difficult to implement. To our knowledge, there is no report of a system to simultaneously

photopolymerize and monitor a photopolymerization reaction in a minimally invasive manner.<sup>23</sup> In certain cases, there is sufficient access to illuminate and monitor polymer injected into a tissue cavity. For instance, in dentistry, while placing a dental implant, a hole is drilled and the tissue cavity can easily be filled and illuminated. The monitoring is done by visual and haptic inspection. In minimally invasive surgery, such as the case of an intervertebral disc replacement, this is more complicated because of the limited space. Having the means to monitor whether the implant is well polymerized is essential: the geometry of the tissue cavity is unknown, tissue pieces can cover the probe tip, or the light can be absorbed by blood. All these issues change the effective polymerization time at each intervention. Therefore, it is necessary to have *in situ* photopolymerization monitoring.

We thus report on a method and device that enables photopolymerization in a minimally invasive way and provides *in situ* monitoring of the photopolymerization state during illumination. We show that the liquid-to-solid transition during photopolymerization can be monitored, which potentially gives the surgeon a real-time feedback during a surgery. We developed a custom surgical probe in which a photoactive material can be (1) mixed, pressurized, and injected, (2) photopolymerized/photoactivated, and (3) monitored during the chemical curing reaction. To illustrate the device performance, we report experiments of hydrogel samples implanted into a bovine intervertebral disc model.

\*Address all correspondence to: Andreas Schmocker, E-mail: [andreas.schmocker@epfl.ch](mailto:andreas.schmocker@epfl.ch)

## 2 In Situ Photopolymerization Monitoring

Figure 1(a) illustrates the probe concept. A cannula or catheter containing an optical light guide is inserted into a living tissue. In the empty space around the optical fiber, a liquid polymer precursor is injected, which flows out to the distal end of the cannula to fill a tissue cavity, such as the degenerated core of an intervertebral disc. The polymer precursor is photopolymerized by light brought by the optical fiber. The photopolymerized solid volume will grow gradually over time. In order to homogenize the light distribution in the volume, scattering particles are added to the photopolymer.<sup>24</sup> In Fig. 1(b), the principle of *in situ* photopolymerization monitoring is illustrated: a second beam of light is sent through the optical light guide. This monitoring light can be reflected, backscattered by the liquid or solid polymer, or the surrounding tissue. The scattering particles further allow collecting photons, which originate from positions outside of the illumination cone of the light guide [e.g., Fig. 1(b), number 3]. This light is then collected by the same light guide and then detected on the proximal side to provide an electronic signal. We expect that the intensity and the spectrum of this signal provide information about the current photopolymerization state in real time and *in situ*.

## 3 Surgical Device for Injection, Illumination, and Monitoring

In Fig. 2, the illumination and detection system as well as the custom surgical probe are presented. The illumination system consists of two arms that are combined by a dichroic, long-pass filter at 400 nm and coupled in a multimode fiber (600  $\mu\text{m}$  core, Polymicon Technologies, FVPE60060710/2M) to provide an illumination source for photopolymerization [light-emitting diode (LED) source at 365 nm, Nichia, NCSU033B] and a source for monitoring the photopolymerization reaction (laser source at 532 nm, CNI Technology, MSL-FN-532). The optical fiber is inserted into the surgical probe (lower right picture). Within the surgical injection probe, the fiber and the liquid polymer-flow are combined. At the distal tip of the probe, the liquid polymer surrounds the fiber flowing in the interspace between the fiber and the cannula wall. A pressurization joint and an integrated Luer-Loc connector ensure that the polymer can be injected at high pressures (up to 50 MPa) without any backflow. During illumination, back-scattered and reflected photons are

collected at the distal end of the illumination fiber and back-propagated through the fiber [as illustrated in Fig. 1(b)]. The dichroic, long-pass filter (550 nm) separates the illumination light from fluorescence and Raman signal generated by the illuminated sample. The band-pass filter (532 nm) filters out the excitation laser light and the spectrometer (Princeton Instruments, Acton SP2300) records the fluorescence and Raman spectra of the sample.

Throughout photopolymerization, the spectrum of the back-scattered light changes. The evolution of the spectrum intensity is described using a function  $F$  that depends on time  $t$  and the wavelength  $\omega$ :

$$F(\omega, t).$$

Let's denote by index  $i$ , the frequency position of the  $i$ 'th spectral peak in the spectrum (e.g., a peak at 600 nm).

$$F_i(t) = F(\omega_i, t).$$

Critical values  $F_{c,i}$  can be defined, which indicate that the photopolymerization reached a critical threshold after time  $T_c$ :

$$F_{c,i} = F(\omega_i, T_c).$$

A critical threshold could be for instance a 90% conversion from uncured precursor to cured network. The polymerization is stopped once such a critical value is reached.

## 4 In Situ Photopolymerization Monitoring Results

Two types of polymer materials were chosen for *in situ* tests: 6 kDa poly(ethylene glycole) dimethacrylate, so called PEGDMA was synthesized,<sup>25</sup> and samples with and without nano-fibrillated cellulose (NFC) fibers (EMPA, Switzerland) were prepared. The cellulose fibers act as scattering particles, which leads to a more uniform distribution of the light in the hydrogel. On the other hand, they also strengthen the polymer-matrix, acting as a reinforcing fiber composite. Irgacure 2959 (BASF, Germany) was used as photoinitiator. The used concentrations are indicated in Table 1.

The tip of the probe was immersed into a large volume of polymer precursor [Fig. 3(a)] and the samples were illuminated

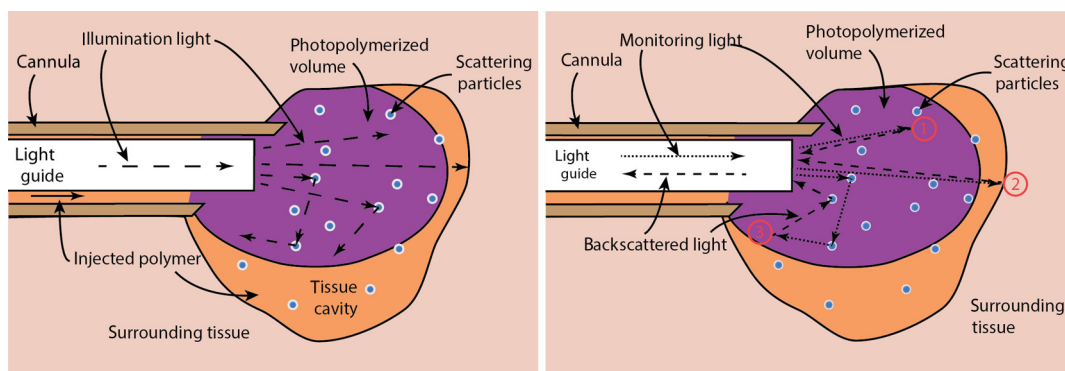


**Fig. 1** Schematic illustration of a probe for (a) *in situ* photopolymerization and (b) *in situ* photopolymerization monitoring. In (a) polymer precursor (orange) is injected into a tissue cavity and illuminated with a UV light for photopolymerization. Scattering particles enhance the amount of photopolymerized polymer (violet) by homogenizing the light in the volume. In (b) a second beam of light is used to monitor the polymerization reaction. This monitoring light can be reflected or backscattered by the polymer directly (1), the surrounding tissue (2), or via the scattering particles (3).

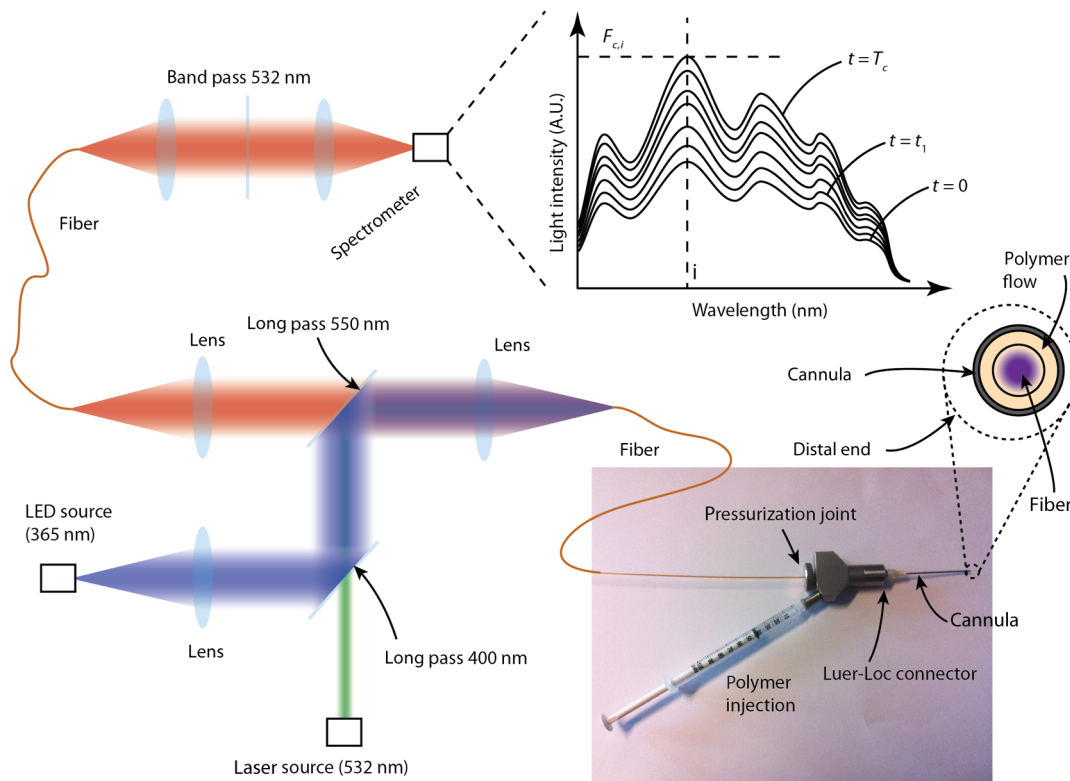


**Fig. 2** Schematic illustration of the illumination and detection system. The sample is illuminated with a light-emitting diode light source (365 nm) to photopolymerize the injected photoreactive precursor and with a green light source (532 nm) to monitor photopolymerization. The spectrometer records the back-scattered fluorescence and Raman spectra. The distal tip of the device consists of a cannula containing the optical fiber and a circular chamber to inject the liquid photopolymer.

with UVA light (365 nm, 3.4 mW) and green light (532 nm, 13.3 mW). A spectrum was recorded every 15 s. To reduce noise, the exposure time was set to 10 s. The experiment was stopped at different time-intervals to evaluate the volume of photopolymerized PEGDMA hydrogel. As a hydrogel is a water-based polymer, the Raman/fluorescence signal of water is used as a reference signal. This signal does not change during the photopolymerization.

As a baseline reference, the spectrum shown in Fig. 3(a) was recorded during immersion of the probe into a phosphate buffer solution (PBS, i.e., water). The first peak at 532 nm is due to the linear scattering and reflections of the excitation beam. Between 532 and 580 nm, the silica Raman bands of the fiber are present with their double peak around 540 nm ( $\sim 450 \text{ cm}^{-1}$ ) and four smaller peaks between 550 and 580 nm ( $\sim 600$  to  $1200 \text{ cm}^{-1}$ ). Between 580 and 700 nm, the signal is dominated by fluorescence. No Raman signal of the water can be seen between 625 and 658 nm ( $2800$  and  $3600 \text{ cm}^{-1}$ ). Between 700 and 780 nm, the spectrum originates from the 365-nm LED itself. In Fig. 3(b), the spectra of a PEGDMA hydrogel during

photopolymerization and monitoring are shown (both the 365 nm LED and the 532 nm laser are turned on). At the beginning (0 min), the spectrum is not significantly different to water. The hydrogel is transparent. No fluorescence is induced. Over time the sample starts to solidify, the spectra gradually change and a strong fluorescence signal centered between 550 and 600 nm appears. A wavelength of 580 nm in the spectrum ( $F_{i=580 \text{ nm}} = f_{580}(t)$ ) was chosen arbitrarily for monitoring the photopolymerization. In Figs. 3(c) and 3(e), a PEGDMA samples without NFC fibers are presented. Hydrogels were illuminated while the fluorescence at 580 nm was monitored. The samples were retrieved and photographed. The samples grew steadily up to a final length of 40 mm after 25 min (after 25 min the polymer growth is limited by the glass container). For the hydrogels without NFC, we observe that the resulting shapes are irregular and the monitoring signal shows peaks appearing between 3 and 5 min. The peaks' positions vary from sample to sample.

The results of the hydrogels with NFC are shown in Figs. 3(d) and 3(f). The resulting shapes are more sphere-like

**Table 1** Preparation of poly(ethylene glycol) dimethacrylate (PEGDMA) hydrogel samples

Sample	PEGDMA 6 kDa [wt%]	Nano-fibrillated cellulose [wt%]	Irgacure 2959 [wt%]	Phosphate buffer solution [wt%]
1. Neat hydrogel	10	0	0.1	89.9
2. Composite hydrogel	10	0.72	0.1	89.18

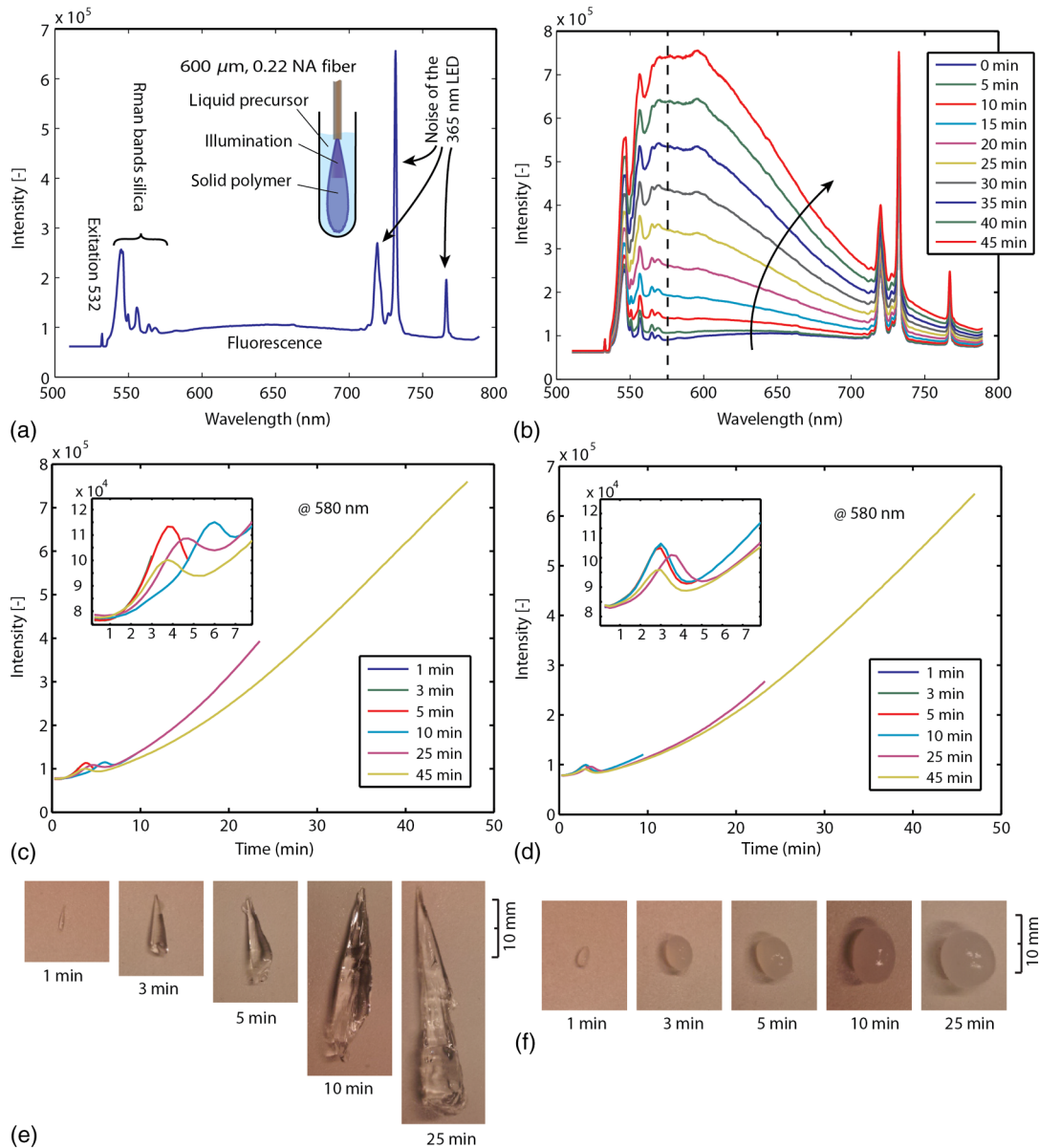


**Fig. 3** Liquid samples were illuminated with a 600  $\mu\text{m}$  fiber. (a) Background signal recorded when immersing the probe into water. (b) Spectra over time during photopolymerization of a poly(ethylene glycol) dimethacrylate (PEGDMA) sample. (c) The change in intensity over time for different samples measured at 580 nm without nano-fibrillated cellulose (NFC) fibers and (d) with NFC fibers. (e) Resulting volumes after photopolymerization without NFC fibers and (f) with NFC fibers

due to the scattering properties of the hydrogel caused by the presence of the nano fibrils of cellulose. The fluorescence intensity curves are reproducible. We observe that the intersample variance of the signal is smaller for the hydrogel with NFC. During photopolymerization, the injected liquid material in front of the probe solidifies first. Thus, its refractive index, particle size, and therefore scattering properties change. A change in the refractive index and a higher amount of scattering events increase the backscattered signal collected by the fiber. This could partly explain the increase in signal around 3 to 5 min; however, it remains unclear why these peaks decrease after this time before growing again.

The particle size can significantly influence the scattering properties of a material. The critical particle size is  $x = 2\pi r/\lambda$ , where  $r$  is the particle diameter and  $\lambda$  the wavelength of

the light. If  $x \ll 1$  is true, Rayleigh scattering will occur. If  $x \sim 1$ , the scattering can be characterized by Mie's theory for spherical particles. Other Mie solutions for different shapes such as infinite cylinders also exist. The size of the NFC fibers has been studied previously using cryo-scanning electron microscopy.<sup>26</sup> However, the results are partially controversial: (1) the fiber size (diameters and length) were not uniform and (2) the fibers also agglomerate. The filament diameter was estimated to be between a few and  $\sim 100$  nm. Therefore, most probably, the occurring scattering is a mixture between Rayleigh and Mie scattering. Moreover, the liquid or solid gel has a white color without any bluish shade, which would occur in the Rayleigh regime (the scattering intensity is proportional to  $1/\lambda^4$ ). This indicates that Mie scattering might be dominant. The hydrogel alone is almost transparent (before, during, and

after photopolymerization). After the photopolymerization of the hydrogel, the NFC fiber network remains incorporated within the hydrogel and the fiber orientation remains unchanged. Therefore, it can be concluded that the scattering properties of the solid or liquid composite hydrogel should be the same.

To better understand how such a polymer develops in time, the *in situ* measured fluorescence signal (via the fiber) was compared to an *ex situ* fluorescence signal (collected from outside of the cuvette). The polymerized volumes induce scattering and fluorescence, which can be recorded from outside the cuvette [Fig. 4(a)]. By applying an intensity threshold to each image [Fig. 4(b)] and counting the pixel values within a relevant area [Fig. 4(c)], the current shape and an *ex situ* intensity are generated. At the same time, the *in situ* fluorescence is measured using the probe [Fig. 4(e)]. No significant change of either the *ex situ* signal or polymerized sample volume could be observed between 2 and 4 min [position of the peak in Fig. 4(e)]. Thus, it can be concluded that the peaks occurring during the 3 to 5 min are not related to the photopolymerized volume.

Furthermore, using the *ex situ* data, the polymer growth is monitored and certain irregularities of the polymer volume are observed, such as shown in Fig. 3(e). In Fig. 4(f), a nucleation is happening locally away from the main volume (red arrow, 5 min). There is an empty or less dense space in between the main volume and the nucleation (red arrow, 5 min and 30 s). Then, the polymer more distal to illumination fiber starts to form (red arrow, 6 min) and only later the empty space is closed (red arrow, 7 min).

In the monitoring experiments shown in Figs. 3 and 4, the fluorescence signal does not exhibit a saturation effect. We

expect that when the hydrogel is fully photopolymerized, the fluorescence signal should saturate. In the experiments above, the volume of the hydrogel was large and the UVA exposure time (up to 50 min) was not enough to fully photopolymerize the whole volume. We thus perform the following experiment with a lower amount of hydrogel and compare the results with photorheology.

In Fig. 5(a), the illuminating fiber was placed at a distance of 500  $\mu\text{m}$  away from the bottom of an optical cuvette [Fig. 5(a)]. To avoid that the precursor dries out or reacts with air during illumination, the cuvette was filled with polymer precursor. Some of the illumination light reaches the volume above the fiber (black arrow) by reflection off the cuvettes' wall and by scattering from the NFC fibers. Finally, the entire volume in the cuvette is cured. Fluorescence photons generated above the fiber tip can still be collected by the same fiber via reflection and scattering (dotted arrow). Figures 5(b) and 5(c) show the cured sample with fiber tip at 365 nm (illumination light) and at 532 nm (monitoring light). Figure 6(d) shows the time dependence the fluorescence spectrum at three monitoring wavelengths. We observe that the signal intensity starts to saturate after approximately 120 min. We then compare this time scale with a photorheology measurement [Fig. 5(e)]. The illumination in the photorheology apparatus is uniform across the area of the hydrogel (illumination intensity: 5  $\text{mW}/\text{cm}^2$ ). The thickness of the hydrogel is 500  $\mu\text{m}$ . The chemical conversion can be associated to the elastic modulus,<sup>27</sup> which is measured using the cyclically rotating plate. The curve saturates after 20 min. The difference in saturation time comes from the illumination geometry. In the case of the fiber, the illumination area is small (0.28  $\text{mm}^2$ ) and light needs to be scattered to reach the

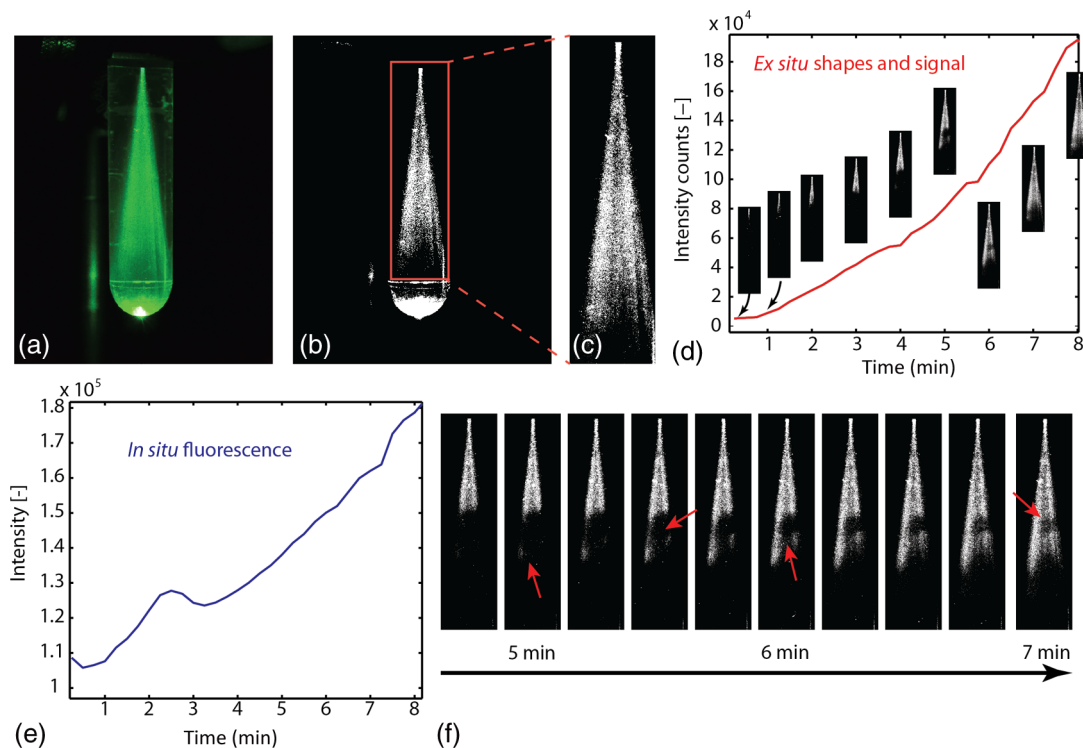


**Fig. 4** The photopolymerized volume is imaged from outside the cuvette (a), a threshold is applied within a relevant area (b) and (c) and by a pixel count the size and the signal intensity plotted over time (d). The *ex situ* signal does not show any peak between 2 and 4 min, while during *in situ* monitoring of the same sample such a peak appears (e). Detail of the evolution of the sample size and geometry over time (f).

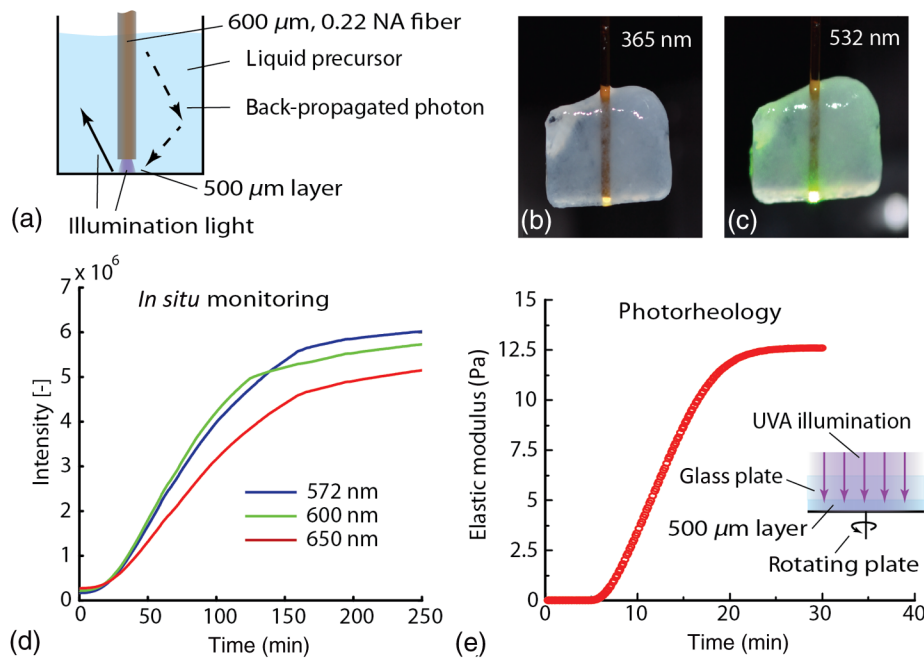


**Fig. 5** Saturation of the monitored fluorescence signal. The fiber tip was placed at 500  $\mu\text{m}$  from the bottom of an optical cuvette containing the liquid poly(ethylene glycol) dimethacrylate-nano-fibrillated cellulose (PEGDMA-NFC) hydrogel (a). The UVA light (b) and visible light (c) are distributed within the entire volume. d) The monitoring signal, measured at three different wavelengths starts to saturate after approximately 120 min. (e) Potorheology of a 500- $\mu\text{m}$  layer of hydrogel to measure the elastic modulus during solidification.

volume whereas in the photorheology apparatus, the whole volume is illuminated with the same intensity at once.

This experiment shows that the fluorescence measurement exhibits a saturation effect that might be attributed to a solidification of the whole volume. However, we cannot exactly monitor a specific conversion state at a given position in the polymer. Figure 5 indicates that the device can still monitor changes of the material, which occur up to 10 mm away from the probe tip only using back-scattered photons. Yet, there is no information about a specific position. The overall collected backscattered fluorescence gives an average over the sample and we correlated the change in fluorescence with the actual polymerized volume. To retrieve more specific information, it would be necessary to emit and collect light at different positions (e.g., using a multicore fiber). Based on the recorded signal and by using a model, for instance Monte Carlo, a conversion rate at a given position could be calculated.

In practice, the surgery time is strongly limited and it would not be possible to illuminate a sample during 120 min. Thus, to further improve the photopolymerization of an injectable implant, either the illumination power can be increased or a more efficient photoinitiator could be used. However, it is also not necessary to achieve a full conversion of the polymer precursor to have sufficient mechanical strength. Conversions of 30% or 50% might already be sufficient to achieve a sufficiently cured material.<sup>28</sup>

As poly(ethylene glycol) (PEG)-base gels usually swell when immersed into water of PBS,<sup>29</sup> the increase in volume could also be attributed to swelling and not photopolymerization. Yet, the impact of dissolved PEG molecules on the ionic strength of the solvent is much higher than the impact of dissolved ions in the PBS ( $\text{Na}^+$ ,  $\text{Cl}^-$ ,  $\text{K}^+$ ,  $\text{PO}_4^{3-}$ , etc.). Therefore, whether PEG is dissolved into water or PBS the

resulting solution will be governed by the PEG-solute. As the hydrophilic PEG backbone is the driving swelling force, the hydrogel swelling will not change throughout the photopolymerization reaction because the PEG backbone itself does not change. Therefore, the osmotic pressure within the solid and the liquid will be the same at any time of the reaction, even independent on whether the hydrogel was prepared with water or PBS. However, this is only true for an isolated system, if the PEG is photopolymerized within a tissue cavity for instance, there will be an osmotic pressure difference between tissue and hydrogel. The hydrogel may attract water from the tissue or vice-versa. In the first case, the hydrogel will swell and exert a pressure onto the cavity wall. The second case results in contraction of the hydrogel and a negative pressure.

## 5 In Vitro Photopolymerization Monitoring

To further evaluate the probe, the poly(ethylene glycol) dimethacrylate-nano-fibrillated cellulose (PEGDMA-NFC) hydrogels were implanted into intervertebral discs. Bovine tails were obtained from a local slaughter house. Following dissection, papain, an enzyme which degenerates the core of the intervertebral disc (IVD), was injected in the IVD (100 to 200  $\mu\text{L}$ , 100 U/mL) and each disc was cultured in an incubator (medium: Dulbecco's Modified Eagle's Medium with 10% Fetal Bovine Serum and 1% L-Glutamine) during 7 days.

The surgeries were performed through a 19 gauge needle (outer diameter: 1.07 mm, inner diameter: 0.69 mm) connected to the probe (Fig. 6). The PEGDMA-NFC hydrogel was injected and then illuminated. During surgery, the position of the needle's tip needs to be located in the middle of the IVD void. If the light-emitting needle tip is covered by a tissue layer, most of the emitted light will be absorbed in the tissue and not in the hydrogel. In Fig. 6(a), an IVD is illuminated at 532 nm

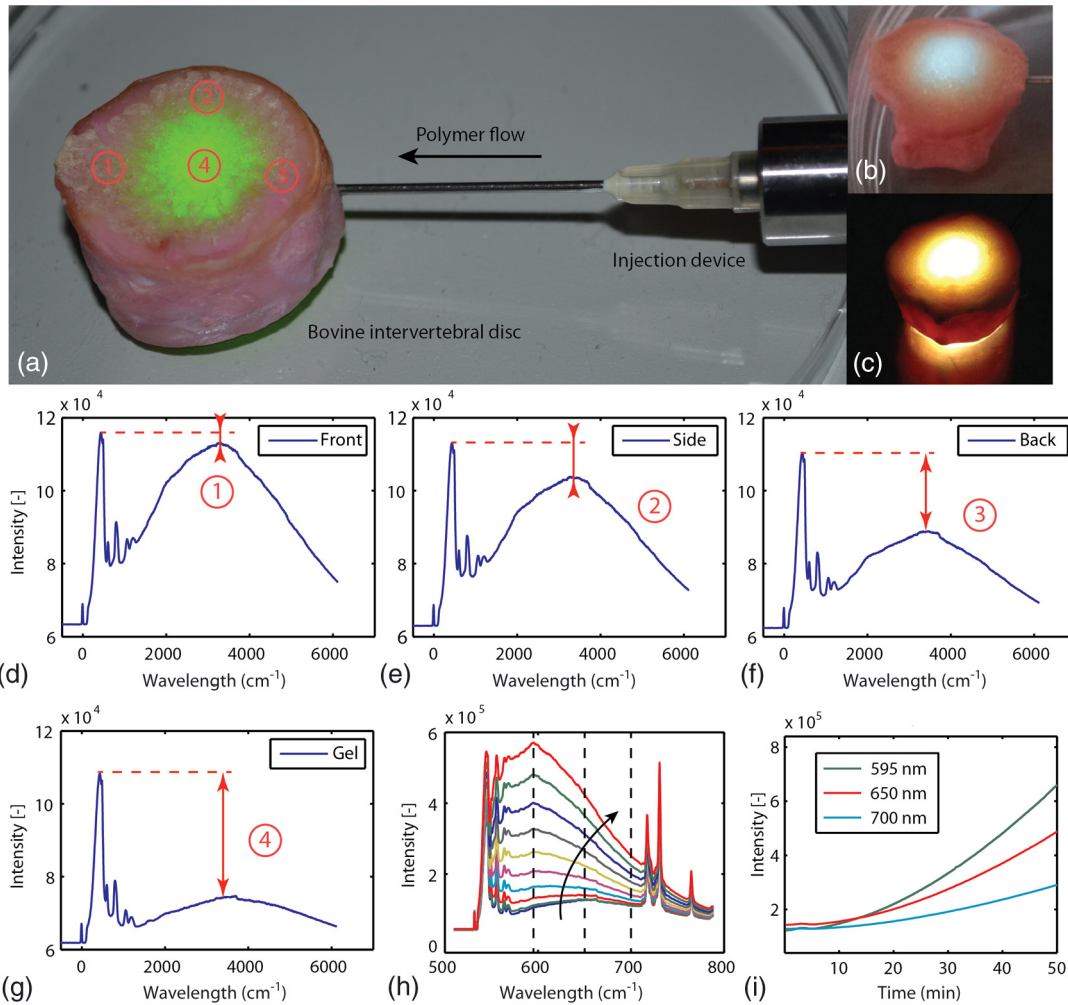


**Fig. 6** PEGDMA hydrogel is injected into a bovine intervertebral disc. (a) The probe is used in a monitoring-only-mode at 532 nm, number (1) to (4) denote different probing positions. (b) and (c) the UVA light (365 nm) is switched on to photopolymerize the injected sample. The different positions (1) to (4) were evaluated: d) at the front of the intervertebral disc, (e) at the side, (f) at the back without hydrogel, and (g) in the middle with hydrogel. (h) *In vitro* photopolymerization monitoring: spectra over time from 0 to 45 min (black arrow). (i) Fluorescence intensity is tracked in function of wavelength over time.

only. This wavelength does not induce any photopolymerization and the space inside the IVD is probed at different positions. If the tip is placed in front of a tissue layer [position 1 and Fig. 6(d)], the scattering is almost as important as the Raman peak of the silica fiber. The signal decreases if the probe is placed at the side of the intervertebral disc [position 2 and Fig. 6(e)] or at the back of the intervertebral disc [position 3 and Fig. 5(f)]. When the PEGDMA hydrogel is injected, tissue scattering is further decreased because the space in front of the tip is filled with the hydrogel [position 4 and Fig. 6(g)]. The hydrogel is then activated by switching on the UVA light [Figs. 5(b) and 5(c)]. Although the tissue scattering background signal is present, the intensity of the backscattered signal develops [Fig. 6(h)] in a similar way as predicted by *in situ* monitoring in a simple cuvette [Fig. 3(d)]. The intensity measured at different wavelengths ( $F_{i=595;600;650 \text{ nm}}$ ) increases steadily, indicating that the injected hydrogel is photopolymerizing [Fig. 5(i)]. The critical value  $F_{c,i}$ , which indicates a given volume of solid hydrogel can be tabulated for a given volume of injected polymer. For instance for a cavity size of 5 mm (diameter),  $F_{c,i}$  would be set at  $1.5 \times 10^5$  [Figs. 3(d) and 3(f)]

assuming that the illumination intensity is kept constant. Another option is to define  $F_{c,i}$  as a relative value such as  $F_{c,relative} = F_{i=595 \text{ nm}}/F_{j=540 \text{ nm}}$ . In this case  $F_{c,relative}$  would be set at  $\sim 0.53$  ( $\sim 2 \times 10^5/3.8 \times 10^5$ ) for the same 5-mm-cavity [Fig. 3(d)]. Look up tables can be integrated into the device architecture and the values can be adapted depending on the size of the cavity or the injected volume, the illumination power, the injected polymer, and the type of surrounding tissue.

## 6 Conclusion

We showed that photopolymerization of PEGDMA can be monitored by fluorescence spectroscopy. Although PEGDMA is transparent to the eye (without NFC) and the used hydrogel solution has a water content of around 90%, the fluorescence light contains enough spectral information that changes as a function of UV illumination time. We have experimentally correlated and quantified the photopolymerized volume growth with the fluorescence signal. It was found that the fluorescence signal increases during the cross-linking reaction. We have demonstrated that the custom probe and transportable photopolymerization monitoring device is functional in an *in vitro* bovine

intervertebral disc. The underlining physics including scattering anisotropies and swelling behavior of the hydrogel during photopolymerization need to be further investigated. This monitoring probe and system could potentially be used as a mean to control the polymerization state for *in situ* and *in vivo* placed implants or drug delivery systems in field of orthopedic or cardiovascular surgery, oncology, or dentistry. This work also shows the need for more effective and faster photoinitiators.

### Acknowledgments

Funding for this research was provided by the Swiss National Fund (#10024003165465).

### References

1. J. S. Owens, "Photopolymerization method," Patent US2344785 (1944).
2. G. Oster, "Dye-sensitized photopolymerization," *Nature* **173**(4398), 300–301 (1954).
3. G. Odian, *Principles of Polymerization*, 4th ed., John Wiley & Sons, Inc., Hoboken, New Jersey (2004).
4. M. Sangermano et al., "One-pot photoinduced synthesis of conductive polythiophene-epoxy network films," *Polymer* **54**(8), 2077–2080 (2013).
5. K. S. Anseth, C. M. Wang, and C. N. Bowman, "Kinetic evidence of reaction diffusion during the polymerization of multi(meth)acrylate monomers," *Macromolecules* **27**(3), 650–655 (1994).
6. H. Zhang et al., "In situ solvothermal synthesis and characterization of transparent epoxy/TiO<sub>2</sub> nanocomposites," *J. Appl. Polym. Sci.* **125**(2), 1152–1160 (2012).
7. K. Ikemura et al., "UV-VIS spectra and photoinitiation behaviors of acylphosphine oxide and bisacylphosphine oxide derivatives in unfilled, light-cured dental resins," *Dent. Mater. J.* **27**(6), 765–774 (2008).
8. B. Sharma et al., "Human cartilage repair with a photoreactive adhesive-hydrogel composite," *Sci. Transl. Med.* **5**(167), 167ra6 (2013).
9. M. P. Lutolf and J. A. Hubbell, "Synthetic biomaterials as instructive extracellular microenvironments for morphogenesis in tissue engineering," *Nat. Biotechnol.* **23**(1), 47–55 (2005).
10. S. J. Bryant, G. D. Nicodemus, and I. Villanueva, "Designing 3D photopolymer hydrogels to regulate biomechanical cues and tissue growth for cartilage tissue engineering," *Pharm. Res.* **25**(10), 2379–2386 (2008).
11. D. A. Wang et al., "Multifunctional chondroitin sulphate for cartilage tissue-biomaterial integration," *Nat. Mater.* **6**(5), 385–392 (2007).
12. Y. An and J. A. Hubbell, "Intraarterial protein delivery via intimately-adherent bilayer hydrogels," *J. Controlled Release* **64**(1–3), 205–215 (2000).
13. J. Vernengo et al., "Synthesis and characterization of injectable bioadhesive hydrogels for nucleus pulposus replacement and repair of the damaged intervertebral disc," *J. Biomed. Mater. Res.* **93**(2), 309–317 (2010).
14. H. M. Simms et al., "In situ fabrication of macroporous polymer networks within microfluidic devices by living radical photopolymerization and leaching," *Lab Chip* **5**(2), 151–157 (2005).
15. J. L. Ifkovits and J. A. Burdick, "Review: photopolymerizable and degradable biomaterials for tissue engineering applications," *Tissue Eng.* **13**(10), 2369–2385 (2007).
16. X. Zhang et al., "In situ monitoring of hydrogel polymerization using speckle interferometry," *J. Phys. Chem. B* **103**(15), 2888–2891 (1999).
17. T. R. McCaffery and Y. G. Durant, "Application of low-resolution Raman spectroscopy to online monitoring of miniemulsion polymerization," *J. Appl. Polym. Sci.* **86**(7), 1507–1515 (2002).
18. S. Kara and Ö. Pekcan, "In situ photon transmission technique for monitoring formation of hydrogels in real-time at various water contents," *Polymer* **41**(16), 6335–6339 (2000).
19. F. W. Wang, R. E. Lowry, and W. H. Grant, "Novel excimer fluorescence method for monitoring polymerization: I. Polymerization of methyl methacrylate," *Polymer* **25**(5), 690–692 (1984).
20. J. Ortyl et al., "Aminophthalimide probes for monitoring of cationic photopolymerization by fluorescence probe technology and their effect on the polymerization kinetics," *Polym. Test.* **31**(3), 466–473 (2012).
21. W. Jager, A. Volkers, and D. Neckers, "Solvatochromic fluorescent probes for monitoring the photopolymerization of dimethacrylates," *Macromolecules* **28**, 8153–8158 (1995).
22. E. Frauendorfer, A. Wolf, and W. D. Hergeth, "Polymerization online monitoring," *Chem. Eng. Technol.* **33**(11), 1767–1778 (2010).
23. K. T. Nguyen and J. L. West, "Photopolymerizable hydrogels for tissue engineering applications," *Biomaterials* **23**(22), 4307–4314 (2002).
24. A. Schmocker et al., "Photopolymerizable hydrogels for implants: Monte-Carlo modeling and experimental in vitro validation," *J. Biomed. Opt.* **19**(3), 35004 (2014).
25. S. Lin-Gibson et al., "Synthesis and characterization of PEG dimethacrylates and their hydrogels," *Biomacromolecules* **5**(4), 1280–1287 (2004).
26. C. Eycholzer et al., "Biocomposite hydrogels with carboxymethylated, nanofibrillated cellulose powder for replacement of the nucleus pulposus," *Biomacromolecules* **12**(5), 1419–1427 (2011).
27. A. Botella et al., "Photo-rheometry/NIR spectrometry: an in situ technique for monitoring conversion and viscoelastic properties during photopolymerization," *Macromol. Rapid Commun.* **25**(12), 1155–1158 (2004).
28. R. Oréface et al., "In situ evaluation of the polymerization kinetics and corresponding evolution of the mechanical properties of dental composites," *Polym. Test.* **22**(1), 77–81 (2003).
29. A. Khoushabi et al., "Photo-polymerization, swelling and mechanical properties of cellulose fibre reinforced poly(ethylene glycol) hydrogels," *Compos. Sci. Technol.* **119**, 93–99 (2015).

**Andreas Schmocker** is a PhD student at the Federal Institute of Technology in Lausanne (EPFL). He received his BS and MS degrees in mechanical, bio-mechanical engineering and management of technology from the same university in 2007 and 2009, respectively. His current research interests include medical- and photonic-device development. He is a winner of a McKinsey award and a member of SPIE and SSBE.

**Christophe Moser** is associate professor of optics. He obtained his PhD at the California Institute of Technology, and co-founded and was CEO of Ondax for 10 years before joining EPFL in 2010. His interests are holography for imaging, endoscopy, head-mounted displays, and optics for solar concentration.

Biographies for the other authors are not available.